Analysis of Filling, Packing, and Cooling Stages in Injection Molding of Disk Cavities

WEN-YEN CHIU, LEO-WANG CHEN, CHI WANG, and DING-CHANG WANG

Department of Chemical Engineering, National Taiwan University, Taipei, Taiwan, Republic of China

SYNOPSIS

This research tried to simulate three stages of injection molding cycles (filling, packing, and cooling) for polypropylene. The cavity used was a center-grated disk-shaped mold. During the filling stage, we assumed the polymer fluid obeyed the CEF equation and flowed nonisothermally. The packing stage was represented by isothermal flow of Newtonian fluid, and, during cooling stage, we took into account the effect of pressure drop on the energy balance. By finite difference method, we could solve the partial differential equations numerically. The results showed: (1) Elastic effect was not significant at the filling stage. (2) Pressure buildup in the cavity was very quick at the packing stage. (3) At the cooling stage, temperatures predicted by taking into account pressure drop were lower than those without considering pressure drop. In addition, the influences of mold temperature, flow rate, and inlet melt temperature on the three stages of injection molding process were discussed.

INTRODUCTION

Injection molding is the most important processing method for plastics. It consists of three stages: (1) filling; (2) packing; (3) cooling. To realize the flow phenomena and thermal history of plastics in mold so as to estimate its microstructure, mechanical properties, and orientation distribution, simulation of these three stages for injection molding is necessary.

Kamal and Kenig[1,2] conducted the simulation of three stages for the semicircular mold. The velocity and temperature distributions of the filling stage and temperature and pressure distributions of the packing and cooling stages were determined by using the finite difference method. For the filling stage, Berger and Gogos,[3] Wu et al.,[4] and Stevenson et al.[5] completed the simulations for the center-gated disk-shaped mold. The work conducted included the relationships among time of filling, thickness of solidified layer, distribution of temperature, flow rate, and pressure drop. Through the method of dimensionless analysis, Stevenson[6] also determined the relationships among pressure drop, clamping force, and dimensionless groups for amorphous plastics in disk-shaped mold. The results could be read very easily by use of a diagram.

The literature for studying the packing stage is sparse: only Kamal and Lafleur[7] simulated the influence of viscoelasticity for a non-Newtonian fluid on packing, by use of the White–Metzner rheological model. Chung and Ide[8] studied the pressure change in the disk-shaped mold for a Newtonian fluid, in which the Spencer–Gilmore state equation was used for compressibility.

As to the cooling stage, Kenig and Kamal[9,10] did simulation on polyethylene. The variations of temperature and pressure for cylindrical-shaped mold with time were determined by use of the finite difference method. The cooling behavior of polyethylene in cylindrical-shaped mold was also realized as the equation of energy was expressed in dimensionless groups. Gutfinger et al.[11] visualized the whole system as a single phase from the concept of Dussinberre's equivalent temperature, which resulted in the 0.5 power relationship between the thickness of solidified layer and time. Moreover, Kamal and Lafleur[12] considered the relationship between heat transfer and nonisothermal crystallization. They also noticed the influence of pressure

Journal of Applied Polymer Science, Vol. 43, 39–48 (1991)
 CCC 0021-8995/91/010039-10$04.00

and heat of crystallization on the equation of energy.[13]

The simulation work for the cycles of injection molding is quite challenging. Many factors influence the flow phenomena of molten plastics, such as viscoelasticity of the polymer, shear rate, temperature, pressure, and heterogeneity of molecular weight, etc. Thus there usually exist certain assumptions: (1) The elasticity of polymer is negligible, (2) It is a non-Newtonian fluid which obeys the power law. (3) No filler is incorporated. Wang et al.[14] pointed out that the power law assumption for polymer fluid was not adequate when the thickness of mold was high or the flow rate was low. They proposed a modified cross model for rectifying the viscosity at low shear rate. They also tried to adopt the CEF equation for examining the viscoelastic effect at isothermal filling for disk-shaped mold. Kamal and Lefleur[12] had analyzed the viscoelastic effect for the filling stage by using the modified Maxwell model.

In this work, the CEF equation was used to examine the viscoelastic effect of PP at nonisothermal filling for disk-shaped mold. The simulation of three stages in the injection cycle was done and discussed in general. The influences of mold temperature, flow rate, and inlet melt temperature on the shear stress, pressure drop, clamping force, and temperature were emphasized.

THEORETICAL TREATMENT

Filling Stage

The mold used for simulation was a center-gated disk-shaped one, which could be visualized as a one-dimensional radial flow. Thus we could assume that:

(1) The thickness of disk was far below its radius.
(2) The gravity, surface tension, fountain effect, and entrance effect were neglected.
(3) Neglecting inertial force, creeping flow was assumed.
(4) The heat conduction in flow direction was neglected.
(5) The fluid was incompressible. All the physical constants except viscosity were fixed. The specifications of the mold were shown in Figure 1.

Assuming the fluid obeyed the CEF[15] (Criminale–Ericksen–Filbey) equation,

$$\tau = -\eta\dot{\gamma} + \tfrac{1}{2}\psi_1 \frac{\vartheta}{\vartheta t}\dot{\gamma} - \tfrac{1}{2}(\psi_1 + 2\psi_2)\{\dot{\gamma}\cdot\dot{\gamma}\} \quad (1)$$

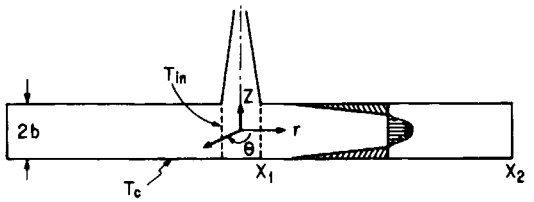

Figure 1 The disk-shaped mold cavity for simulation.

in which $\vartheta/\vartheta t$ was corotational derivative. As usual, ψ_2 was much smaller than ψ_1, and its value was negative. If we assumed $\psi_2 = 0$, then eq. (1) became

$$\tau = -\eta\dot{\gamma} + \tfrac{1}{2}\psi_1\left(\frac{\vartheta}{\vartheta t}\dot{\gamma} - \{\dot{\gamma}\cdot\dot{\gamma}\}\right) \quad (2)$$

In the thin disk mold, the velocity could be expressed as

$$V_r = V_r(r, z, t), \quad V_\theta = V_z = 0$$

Assuming a quasisteady state, then $(\partial/\partial t)\dot{\gamma} = 0$. After simplification, the components of τ were obtained:

$$\tau_{rr} = -2\eta\frac{\partial V_r}{\partial r} + \psi_1\left[V_r\frac{\partial^2 V_r}{\partial r^2} - 2\left(\frac{\partial V_r}{\partial r}\right)^2 - \left(\frac{\partial V_r}{\partial z}\right)^2\right] \quad (3)$$

$$\tau_{\theta\theta} = -2\eta\frac{V_r}{r} + \psi_1\left[V_r\frac{\partial}{\partial r}\left(\frac{V_r}{r}\right) - 2\left(\frac{V_r}{r}\right)^2\right] \quad (4)$$

$$\tau_{rz} = \tau_{zr} = -\eta\frac{\partial V_r}{\partial z} + \frac{1}{2}\psi_1\left[V_r\frac{\partial^2 V_r}{\partial r\,\partial z} - \frac{\partial V_r}{\partial r}\cdot\frac{\partial V_r}{\partial z}\right] \quad (5)$$

$$\tau_{zz} = \tau_{\theta r} = \tau_{r\theta} = \tau_{\theta z} = \tau_{z\theta} = 0 \quad (6)$$

Wang et al.[14] of Cornell University used the CEF equation instead of the GNF equation to find out the influence of normal stress on pressure drop under the isothermal flow condition. He achieved the following conclusion: "For filling behavior of disk-shaped mold under isothermal condition, the pressure drop predicted by taking into account the normal stress effect is 5% lower than that without considering the normal stress effect, hence this effect was negligible." Thus equation of motion could be written as

$$\frac{\partial p}{\partial r} = -\frac{\partial \tau_{rz}}{\partial z} \quad (7)$$

Nevertheless, the high speed of filling behavior for general plastics could induce significant viscous heat, which resulted in temperature rise, viscosity drop, and pressure drop. The error might be huge if only isothermal filling was considered. The effect of normal stress in the equation of energy is the task studied in this work.

The equation of energy

$$\rho C_p\left(\frac{\partial T}{\partial t} + V_r\frac{\partial T}{\partial r}\right) = -\frac{\partial q_z}{\partial z} - \left(\tau_{rr}\frac{\partial V_r}{\partial r} + \tau_{\theta\theta}\frac{V_r}{r}\right) - \tau_{rz}\frac{\partial V_r}{\partial z} \quad (8)$$

We introduced eqs. (3) and (4) into (8), and assumed that the flow rate was constant. After simplification, we get

Equation of continuity:

$$Q = 2\pi\int_{-b}^{b} r\,Vr\,dz = 2\pi\int_{-b}^{b} f(z)\,dz \quad (9)$$

Equation of motion:

$$\frac{\partial p}{\partial r} = \frac{\partial}{\partial z}\left(\eta\frac{\partial V_r}{\partial z}\right) \quad (10)$$

Equation of energy:

$$\rho C_p\left(\frac{\partial T}{\partial t} + V_r\frac{\partial T}{\partial r}\right) = K\frac{\partial^2 T}{\partial z^2} + \left(\eta - \psi_1\frac{V_r}{r}\right)\left(\frac{\partial V_r}{\partial z}\right)^2 \quad (11)$$

Boundary conditions:

1. $\dfrac{\partial V_r(r, z = 0, t)}{\partial z} = 0.$
2. $V_r(r, z = b, t) = 0.$
3. $T(r = x_1, z, t) = T_{\text{in}}.$
4. $T(r, z = b, t) = T_c.$
5. $(\partial T/\partial r)(r = X_{\text{int}}, z, t) = 0$, where $X_{\text{int}} = X$ at the melt front, i.e., the thermal insulation was approximated at the boundary of melt front and atmosphere.

For polypropylene, the cross model was used for expressing the viscosity:

$$\eta(\dot\gamma, T) = \frac{\eta_0(T)}{1 + C[\eta_0(T)\dot\gamma]^{1-n}},$$

$$\text{where } \eta_0\cdot(T) = B\exp(T_b/T) \quad (12)$$

If $T < 440$ K, then $\eta(\dot\gamma, T) = \eta_0(T)$ by definition,

$$\psi_1 = \frac{\tau_{11} - \tau_{22}}{\dot\gamma^2}$$

From Chiu and Shyu's work,[16] we knew

$$\psi_1 = 1.75 \times 10^5\dot\gamma^{0.026-2} \quad \text{for PP at 180°C} \quad (13)$$

$$\eta = 1.20 \times 10^5\dot\gamma^{0.5-1} \quad \text{for PP at 180°C} \quad (14)$$

Then from eqs. (13) and (14), we got the principle normal stress difference

$$N_1 = \tau_{11} - \tau_{22} = 2.264 \times 10^{-5}\tau_{12}^{1.947} \quad (15)$$

The relationship between N_1 and τ_{12} in eq. (15) was found to hold at any temperatures.[17]

Equations (9)–(11) were solved by the finite difference method to obtain the velocity profile, pressure profile, and temperature distribution. By utilizing the iteration method, we proceeded with fluid with one step in the r-direction whenever the relative error between the new and old values of pressure was less than 5%. The work was continued until the mold was filled.

Packing Stage

Refering to Chung's[8] theoretical analysis, the following assumptions were proposed:

(1) The flow in the mold was isothermal.
(2) It was Newtonian fluid.
(3) The inertial force, gravity, and elastic effect were neglected.
(4) The fluid obeyed the Spencer–Gilmore state equation, which meant

$$(P + W)\left(\frac{1}{\rho} - \frac{1}{\rho_0}\right) = R_c T \quad (16)$$

where P = pressure, T = temperature, ρ = density, and W, ρ_0, and R_c were empirical constants.

The isothermal assumption in the packing stage was reasonable due to the extremely short time interval, which meant that the temperature of fluid could maintain at that interval of the end of filling stage. The deformation rate and viscous heat were very small; therefore, the assumption of Newtonian fluid was made in the packing stage.

Equation of continuity:

$$\frac{\partial\rho}{\partial t} - \frac{1}{r}\frac{\partial}{\partial r}(\rho_r V_r) = 0 \quad (17)$$

Equation of motion:

$$\frac{\partial p}{\partial r} = \eta \frac{\partial^2 V_r}{\partial z^2}. \tag{18}$$

Boundary conditions:

$$V_r(r, z = b, t) = 0$$

$$\frac{\partial V_r}{\partial z}(r, z = 0, t) = 0$$

From above equations, we got

$$V_r(r, z) = \frac{1}{2\eta}\left(-\frac{\partial p}{\partial r}\right)(b^2 - z^2) \tag{19}$$

By using eq. (16), we replaced $(\partial p/\partial r)$ in eq. (19) by $(\partial \rho/\partial r)$, which yielded

$$V_r(r, z) = \frac{1}{2\eta}\frac{R_c T \rho_0^2}{(\rho_0 - \rho)^2}\left(-\frac{\partial \rho}{\partial r}\right)(b^2 - z^2) \tag{20}$$

Introduced eq. (20) into eq. (17), which yielded

$$\frac{\partial \rho}{\partial t} - \frac{(b^2 - z^2)\rho_0^2 R_c T}{2\eta}\left[\frac{\rho}{r(\rho_0 - \rho)^2}\frac{\partial \rho}{\partial r} + \frac{\rho_0 + \rho}{(\rho_0 - \rho)^3} \times \left(\frac{\partial \rho}{\partial r}\right)^2 + \frac{\rho}{(\rho_0 - \rho)^2} \times \frac{\partial^2 \rho}{\partial r^2}\right] = 0 \tag{21}$$

Initial condition:

$$t = 0, \quad \rho = \rho_{\text{fill}}(r, z)$$

which means that the final density distribution of filling stage could be taken as the initial condition of packing stage.

Boundary conditions:

1. $t > 0$ at $r \le X_1$, $\rho = \rho_{\text{given}}(t)$ or $P = F(t)$.
2. $t > 0$ at $r = X_2$, $(\partial \rho/\partial r) = 0$.

We wrote eq. (21) into an implicit finite difference form, and solved the equation with the iteration method, in which the convergent condition was that one could proceed with the time with one interval whenever the difference between the new and old values of density was less than 10^{-4} g/cm^3. The pressure distributions in r- and z-directions and the velocity distribution could also be determined. The mass flow rate could be obtained from the velocity distribution over z. Through the integration of mass flow rate over time, the total amount of PP injected into the mold during the packing stage could be calculated.

For polypropylene, the constants in the Spencer–Gilmore equation were assigned as

$$W = 2146.26 \text{ kg/cm}^2$$

$$\rho_0 = 1.02 \text{ g/cm}^3$$

$$R_c = 1.589 \text{ kg cm/g K}$$

Cooling Stage

The simulation of 1-dimensional heat-transfer analysis for the disk mold was conducted primarily based on Dietz's[18] theoretical analysis. It was assumed that the heat-transfer took place only in the z-direction, so that the heat transferred per unit mass was

$$dq = C_p\, dT - T\left(\frac{\partial V}{\partial T}\right)_p dP \tag{22}$$

At a very short interval

$$\frac{\partial q}{\partial t} = C_p \frac{\partial T}{\partial t} - T\left(\frac{\partial V}{\partial T}\right)_p \frac{\partial p}{\partial t} \tag{23}$$

The fluid was assumed at rest during cooling stage, the pressures everywhere were equal. Then

$$\frac{\partial p}{\partial t} = \frac{dp}{dt}$$

For every small mass dm,

$$\dot{Q}_{\text{in}} - \dot{Q}_{\text{out}} = d\dot{Q} = \pi X_2^2\left[-K\frac{\partial T}{\partial z}\bigg|_z + K\frac{\partial T}{\partial z}\bigg|_{z+\Delta z}\right] = \pi X_2^2 \frac{\partial}{\partial z}\left(K\frac{\partial T}{\partial z}\right) dz \tag{24}$$

and

$$d\dot{Q} = \frac{\partial (dm \cdot q)}{dt} = dm\frac{\partial q}{\partial t} = \pi X_2^2\, dz\, \rho \frac{\partial q}{\partial t} \tag{25}$$

Comparing eq. (24) with (25), we found

$$\frac{\partial q}{\partial t} = \frac{1}{\rho}\frac{\partial}{\partial z}\left(K\frac{\partial T}{\partial z}\right) \tag{26}$$

Table I Thermal Physical Properties and the Parameters of Viscosity in Cross Model for PP

n	0.323
T_b (K)	4.55×10^3
B (g/cm s)	9.0
C [(g/cm s^2)$^{n-1}$]	3.77×10^{-4}
ρ (g/cm^3)	0.77
K (cal/cm s K)	3.6×10^{-4}
C_p (cal/g K)	0.65

Introducing eq. (26) into (23) and simplifying, we got

$$\rho C_p \frac{\partial T}{\partial t} = K\left[\frac{\partial^2 T}{\partial z^2} + \frac{1}{K}\left\{\left(\frac{\partial K}{\partial z}\right)\left(\frac{\partial T}{\partial z}\right) + \frac{T}{V}\left(\frac{\partial V}{\partial T}\right)_p \frac{dp}{dt}\right\}\right] \quad (27)$$

Initial condition:

$$t = 0, \quad T(z) = T_{\text{fill}}(z)$$

which meant that the average value of final temperatures in the r-direction for the filling stage was taken as the initial condition for the cooling stage.

Boundary conditions:

1. $t > 0$, at $z = 0$, $[\partial T(z)/\partial z] = 0$.
2. $t > 0$, at $z = b$, $T(z = b) = T_{\text{wall}}$.

We converted eq. (27) into an implicit finite difference form, and solved it with the iteration method. The convergent condition was that one could proceed with the time with one interval only when the temperature difference between the new and old values was less than 0.1°C.

RESULTS AND DISCUSSIONS

The thermal physical constants and the parameters of viscosity of PP in the cross model for the simulation of the injection molding process are shown in Table I.

Filling Stage

The thickness of the disk for simulation was either 0.254 or 0.406 cm, the diameter of entrance sprue was 0.66 cm, and the radius of disk was 10.16 cm. First, the GNF model was used for simulating the pressure drop, which resulted in the values within 5% errors in comparison with those simulated by Wang.[14] Further, simulation by the CEF model was conducted. The results are shown in Table II. From the small difference between these two simulations, we confirmed that the normal stress induced by shear flow was negligible for the disk mold.

The inlet temperature of the fluid was kept at 500 K, the flow rate was 400 cm^3/s, the thickness of mold was 0.254 cm, and the mold temperature was 311 K. Simulation was conducted under the abovementioned conditions, from which the flow profile in the filling stage for PP was studied.

Figure 2 shows the temperature distribution, in the radial direction. The temperature continuously rose along the flow (r) direction, which exhibited the effect of viscous heat for PP. Figure 3 shows the temperature distribution in the thickness direction.

Table II The Effect of Normal Stress Due to Shear Flow on the Q–Π_{zz}[a] Relation for Radial Flow

Π_{zz} \ Q	50 cm^3/s	100 cm^3/s	200 cm^3/s	300 cm^3/s	400 cm^3/s
		b = 0.127 cm			
GNF eq. (dyn/cm^2)	9.212E7	8.536E7	8.776E7	9.110E7	9.422E7
CEF eq. (dyn/cm^2)	9.218E7	8.541E7	8.785E7	9.121E7	9.436E7
		b = 0.203 cm			
GNF eq. (dyn/cm^2)	3.719E7	3.608E7	3.820E7	4.024E7	4.319E7
CEF eq. (dyn/cm^2)	3.724E7	3.609E7	3.822E7	4.026E7	4.322E7

[a] Π_{zz} = pressure drop (r = 1.91–10.16 cm) at the end of filling stage.

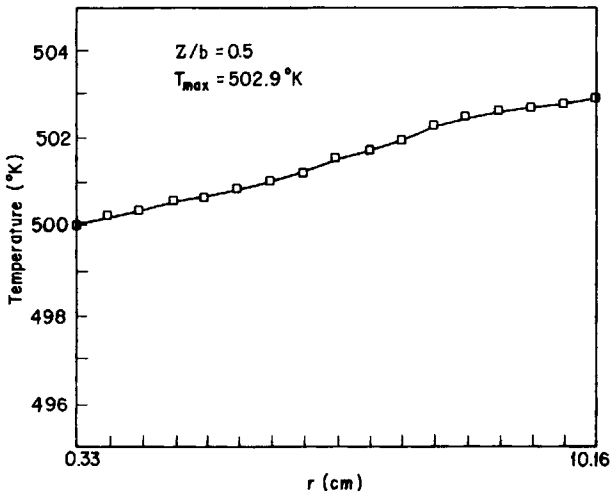

Figure 2 Temperature profile in the r-direction.

The temperatures in the core area of the mold were mostly kept at the same as inlet temperature. However, the temperature dropped sharply in the skin area. The velocity distribution in the thickness direction is shown in Figure 4, from which we knew that the fluid was frozen into solid whenever z/b was above 0.9; thus the velocity was zero. Figure 5

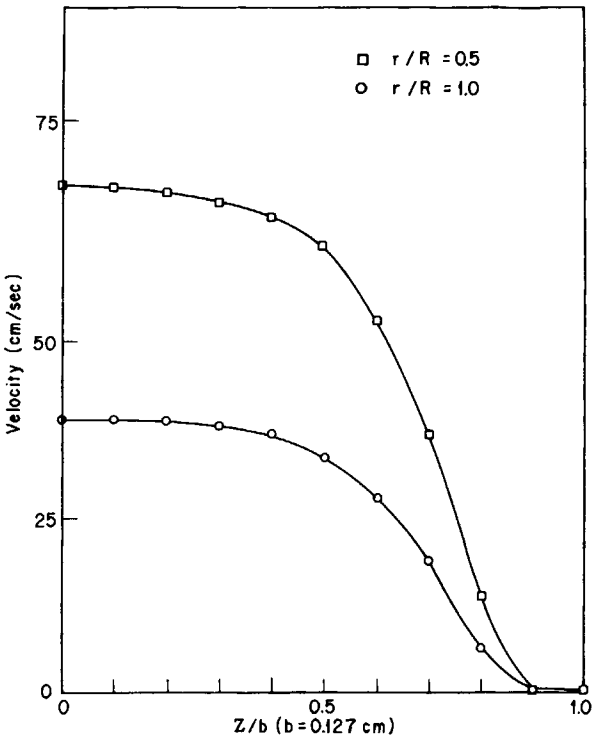

Figure 4 Velocity profile in the z-direction.

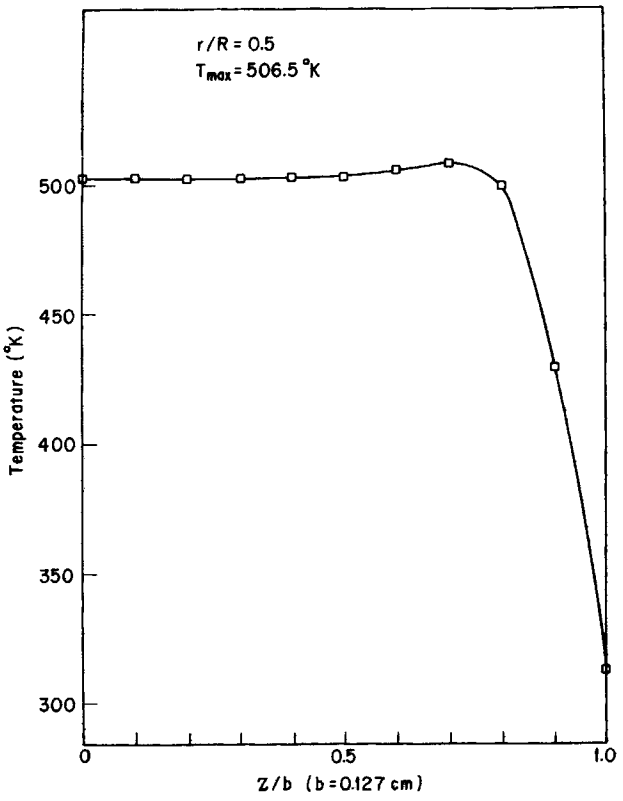

Figure 3 Temperature profile in the z-direction.

shows the relationship between velocity and time for different r values. Since the variation of velocity versus time was very small, the assumption of quasi-steady-state on velocity was reasonable. Figure 6 shows the shear rate distribution in the thickness direction, which revealed that the larger the radius, the lower the shear rate. Figure 7 shows the shear stress distribution in the thickness direction, in which the maximum shear stress occurred at $z/b = 0.8$. The larger the radius, the lower the shear stress. Figure 8 shows the thickness of solid layer at different filling conditions. The lower fluid temperature gave a thicker solid layer, and this effect was the most prominent. The smaller flow rate resulted in a thicker solid layer due to the higher cooling effect. The influence of mold temperature was of minor significance.

Packing Stage

The final pressure of the filling stage was taken as the initial condition of packing stage. The distribution of pressure could be converted into the distribution of density by the Spencer–Gilmore model. The results are shown in Figure 9, from which we knew that the pressure drop was the highest near the entrance. The pressure in the mold increased

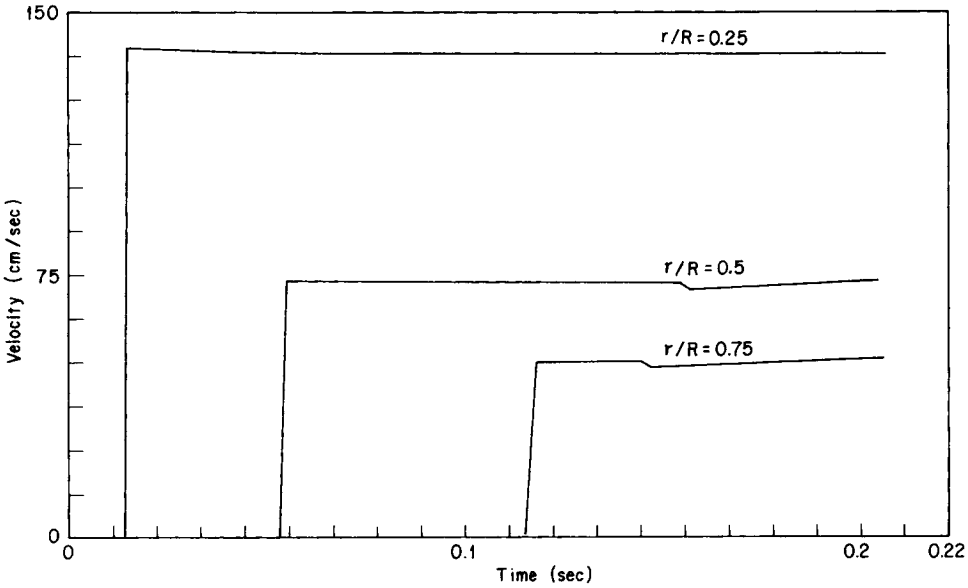

Figure 5 Variation of velocity with time at $z = 0$.

and gradually became homogeneous with time. At the start of the packing stage, the quantity of fluid flowing into the area near the entrance was lower than that flowing out because of the radial flow. For this reason, the pressure dropped slightly at the entrance. When the pressure became more homogeneous, this phenomenon disappeared. Pressure rose very fast from that time, and the pressures in the mold became almost homogeneous within as short a time as 0.2 s.

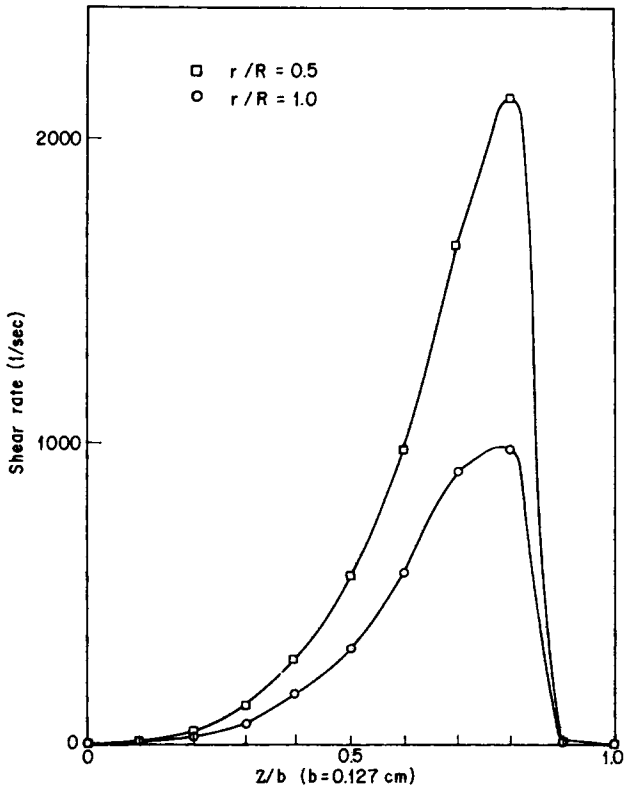

Figure 6 Shear rate profile in the z-direction.

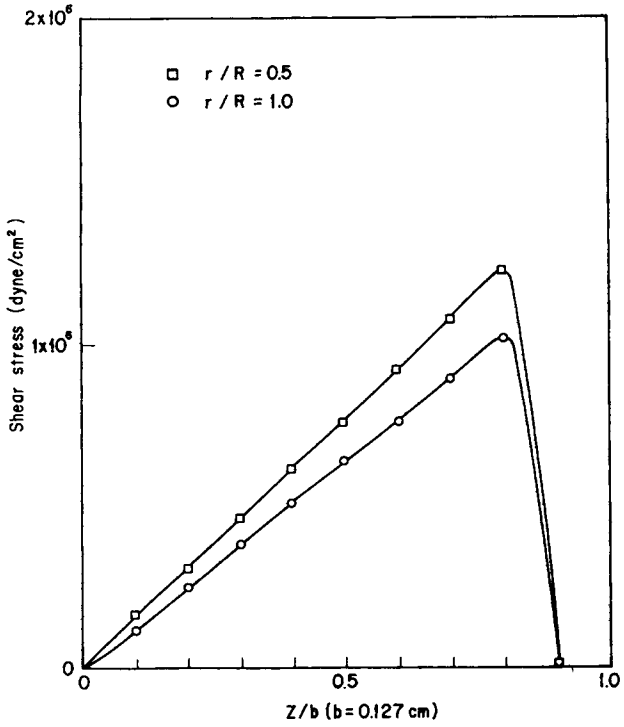

Figure 7 Shear stress profile in the z-direction.

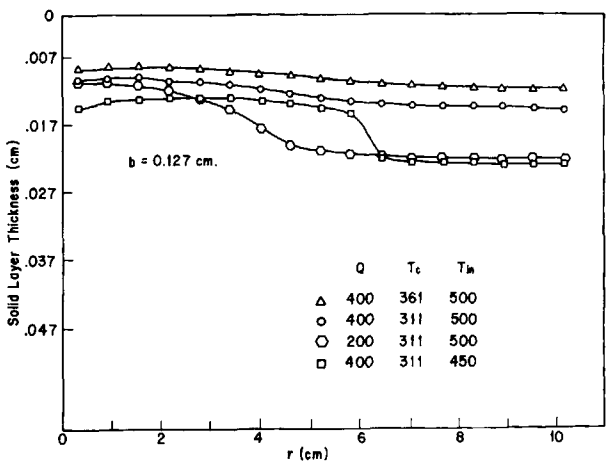

Figure 8 "Frozen skin" profile for different filling conditions.

Cooling Stage

It was assumed that the pressures everywhere in the mold were the same for the cooling stage. The variations of pressure with time could be expressed as follows:

$$P = 4500 - (4500/6)t \quad \text{(psi)}, \quad t \leq 6 \text{ s}$$

$$P = 0 \quad \text{(psi)}, \quad t > 6 \text{ s}$$

which meant that the final pressure of the packing stage (4500 psi) was taken as the initial pressure of the cooling stage. The pressure dropped to atmosphere at 6 s.

Figure 10 shows the variation of temperature with time, where z/b equals 0.5. The temperature which took into account the influence of pressure on the equation of energy was lower than that without considering its influence. The largest difference between these two temperature profiles was about 0.6°C.

In all, the influences of mold temperature, flow rate, and inlet melt temperature on the three stages of the injection molding process were examined in this work; the results are shown in the following tables:

Table III showed the influence of mold temperature: The higher the mold temperature, the lower the maximum shear stress, pressure drop, and clamping force would be; but the quantity of fluid injected into the mold at packing stage was higher.

Table IV showed the influence of flow rate: The higher the flow rate, the more significant the viscous-heat effect and the higher the maximum temperature and maximum shear stress would be, whereas the pressure drop and clamping force decreased first and then increased. This came from the fact that the cooling effect of the mold was more significant at a lower flow rate. In addition, the quantity of fluid injected at the packing stage increased when the flow rate increased.

Table V showed the influence of inlet temperature of the fluid: The higher the inlet melt temperature, the smaller the maximum shear stress, pressure

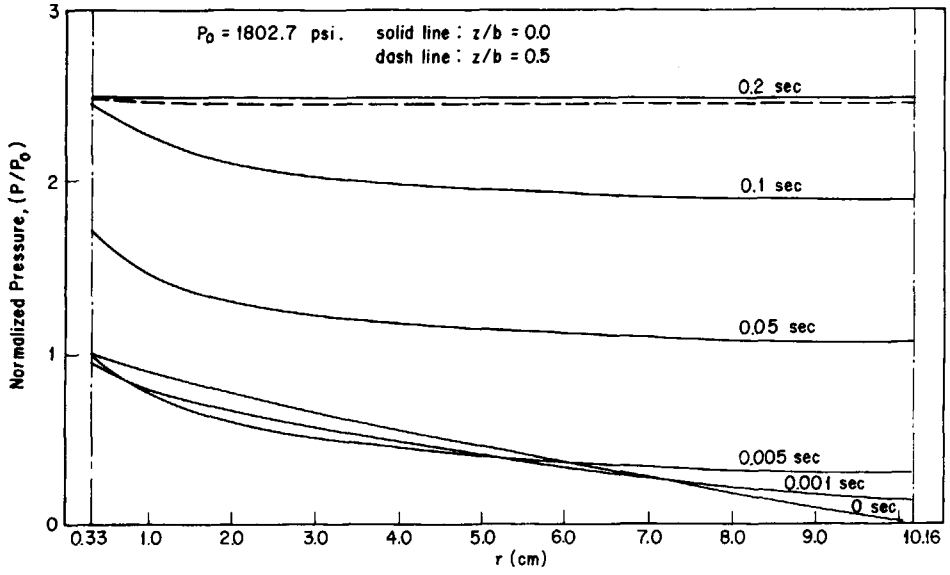

Figure 9 Pressure buildup in the disk cavity for polypropylene during the packing stage.

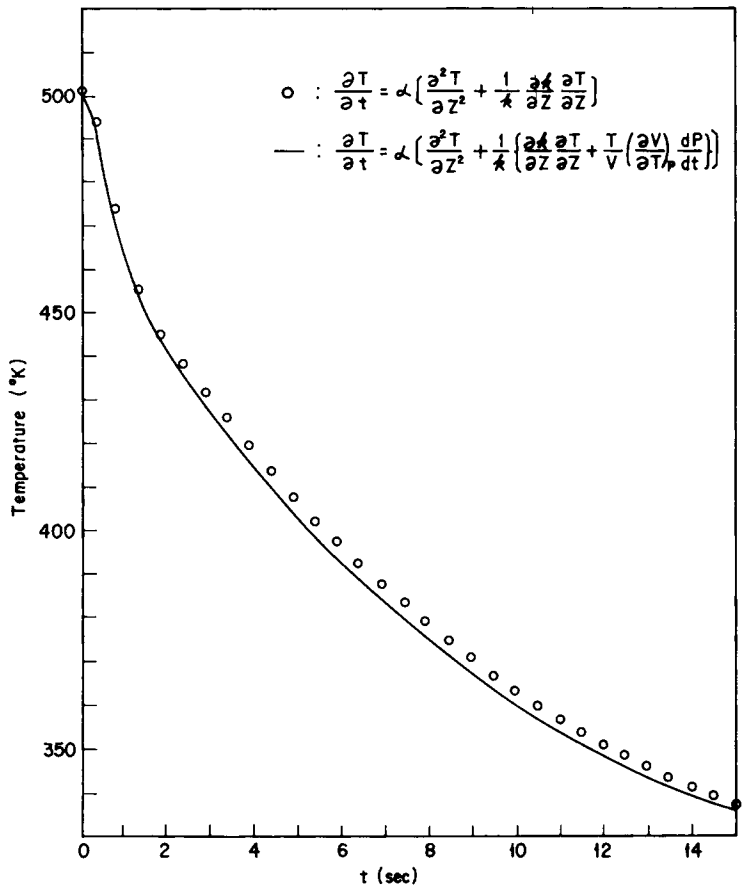

Figure 10 Temperature vs. time for $z/b = 0.5$ during cooling stage.

drop, and clamping force would be, whereas the quantity of fluid injected into the mold at packing stage was higher.

CONCLUSION

The simulation of injection molding cycles for the disk mold for PP informed us that:

(1) At the filling stage, the elastic effect of polymer was negligible.
(2) At the packing stage, the buildup of pressure was very fast.
(3) At the cooling stage, the temperature predicted by taking into account the influence of the pressure drop on the equation of energy was lower than that without considering its influence.

Table III Simulation Results for Different Mold Temperatures[a]

T_c (K)	T_{max} (K)	τ_{max} (dyn/cm^2)	Π_{zz} (dyn/cm^2)	F (dyn)	Filling Time (s)	Mass (g)
286	503.0	2.647×10^6	8.871×10^7	1.107×10^{10}	0.411	1.326
311	502.9	2.638×10^6	8.650×10^7	1.082×10^{10}	0.411	1.328
336	502.9	2.626×10^6	8.401×10^7	1.053×10^{10}	0.411	1.331

[a] T_{max} = max temp in the cavity during filling stage; τ_{max} = max shear stress in the cavity during filling stage; Π_{zz} = pressure drop between $r = 1.91$ and 10.16 cm at the end of filling stage; F = clamp force required at the end of filling stage; mass = total mass flow into the cavity during packing stage; Q = volumetric flow rate = 200 cm^3/s; T_{in} = inlet melt temperature = 500 K.

Table IV Simulation Results for Different Volumetric Flow Rates[a]

Q (cm^3/s)	T_{max} (K)	τ_{max} (dyn/cm^2)	Π_{zz} (dyn/cm^2)	F (dyn)	Filling Time (s)	Mass (g)
50	500.5	1.678×10^6	8.312×10^7	1.104×10^{10}	1.646	1.316
100	501.3	2.105×10^6	8.275×10^7	1.061×10^{10}	0.823	1.325
200	502.9	2.638×10^6	8.650×10^7	1.082×10^{10}	0.411	1.328

[a] T_{in} = inlet melt temperature = 500 K; T_c = mold temperature = 311 K. See footnote to Table III for the meaning of the other symbols.

Table V Simulation Results for Different Inlet Melt Temperatures[a]

T_{in} (K)	T_{max} (K)	τ_{max} (dyn/cm^2)	Π_{zz} (dyn/cm^2)	F (dyn)	Filling Time (s)	Mass (g)
475	479.3	3.108×10^6	10.18×10^7	1.275×10^{10}	0.411	1.163
500	502.9	2.638×10^6	8.650×10^7	1.082×10^{10}	0.411	1.328
525	527.2	2.278×10^6	7.503×10^7	0.939×10^{10}	0.411	1.492

[a] Q = volumetric flow rate = 200 cm^3/s; T_c = mold temperature = 311 K. See footnote to Table III for the meaning of the other symbols.

REFERENCES

1. M. R. Kamal and S. Kenig, *Polym. Eng. Sci.*, **12,** 294 (1972).
2. M. R. Kamal and S. Kenig, *Polym. Eng. Sci.*, **12,** 302 (1972).
3. J. L. Berger and C. G. Gogos, *Polym. Eng. Sci.*, **13,** 102 (1973).
4. P. C. Wu, C. F. Huang, and C. G. Gogos, *Polym. Eng. Sci.*, **14,** 223 (1974).
5. J. F. Stevenson, A. Galskoy, and K. K. Wang, *Polym. Eng. Sci.*, **17,** 706 (1977).
6. J. F. Stevenson, *Polym. Eng. Sci.*, **18,** 577 (1978).
7. M. R. Kamal and P. G. Lafleur, *SPE ANTEC Tech. Pap.*, **29,** 386 (1983).
8. T. S. Chung and T. Ide, *J. Appl. Polym. Sci.*, **28,** 2999 (1983).
9. S. Kenig and M. R. Kamal, *SPE J.*, **26,** 50 (1970).
10. S. Kenig and M. R. Kamal, *Can. J. Chem. Eng.*, **49,** 210 (1971).
11. C. Gutfinger, E. Bryer, and Z. Tadmor, *Polym. Eng. Sci.*, **15,** 515 (1975).
12. M. R. Kamal and P. G. Lafleur, *Polym. Eng. Sci.*, **24,** 692 (1984).
13. M. R. Kamal and P. G. Lafleur, *Polym. Eng. Sci.*, **22,** 1066 (1982).
14. K. K. Wang et al., Cornell University, 1975–1979.
15. R. B. Bird, R. C. Armstrong, and Q. Hassager, *Dynamics of Polymeric Liquids,* John Wiley & Sons, New York 1977, Vol. 1.
16. W. Y. Chiu and G. D. Shyu, *J. Appl. Polym. Sci.*, **35,** 847 (1988).
17. W. Minoshima, J. L. White, and J. E. Spruiell, *Polym. Eng. Sci.*, **20,** 1166 (1980).
18. W. Dietz, *Polym. Eng. Sci.*, **18,** 1030 (1978).

Received June 15, 1990
Accepted November 9, 1990